J. Membrane Biol. 161, 247–256 (1998)

The Journal of
Membrane
Biology

Membrane Potassium Channels and Human Bladder Tumor Cells. I. Electrical Properties

S.H. Monen, P.H. Schmidt, R. Wondergem

Department of Physiology, James H. Quillen College of Medicine, East Tennessee State University, Johnson City, TN 37614-0576, USA

Received: 12 June 1997/Revised: 21 October 1997

Abstract. These experiments were conducted to determine the membrane K^+ currents and channels in human urinary bladder (HTB-9) carcinoma cells in vitro. K^+ currents and channel activity were assessed by the whole-cell voltage clamp and by either inside-out or outside-out patch clamp recordings. Cell depolarization resulted in activation of a Ca^{2+}-dependent outward K^+ current, 0.57 ± 0.13 nS/pF at −70 mV holding potential and 3.10 ± 0.15 nS/pF at 30 mV holding potential. Corresponding patch clamp measurements demonstrated a Ca^{2+}-activated, voltage-dependent K^+ channel (K_{Ca}) of 214 ± 3.0 pS. Scorpion venom peptides, charybdotoxin (ChTx) and iberiotoxin (IbTx), inhibited both the activated current and the K_{Ca} activity. In addition, on-cell patch recordings demonstrated an inwardly rectifying K^+ channel, 21 ± 1 pS at positive transmembrane potential (V_m) and 145 ± 13 pS at negative V_m. Glibenclamide (50 μM), Ba^{2+} (1 mM) and quinine (100 μM) each inhibited the corresponding nonactivated, basal whole-cell current. Moreover, glibenclamide inhibited K^+ channels in inside/out patches in a dose-dependent manner, and the IC_{50} = 46 μM. The identity of this K^+ channel with an ATP-sensitive K^+ channel (K_{ATP}) was confirmed by its inhibition with ATP (2 mM) and by its activation with diazoxide (100 μM). We conclude that plasma membranes of HTB-9 cells contain the K_{Ca} and a lower conductance K^+ channel with properties consistent with a sulfonylurea receptor-linked K_{ATP}.

Key words: Patch Clamp — Calcium — ATP — Glibenclamide — Charybdotoxin — Iberiotoxin

Introduction

Potassium conductance of the plasma membrane is a major determinant of the resting membrane potential in eukaryotic cells. It also plays an important functional role in regulating cell growth (Nilius & Wohlrab, 1992), cytokine secretion (Chandy et al., 1984), the cell cycle (Amigorena et al., 1990), and cell volume (Grinstein & Foskett, 1990), along with a well-established role in many excitable cells of repolarizing the membrane during action potentials.

The membrane potassium conductance comprises currents carried by various K^+ channels. These are grouped into three families that differ by the number (either six, two or one) of membrane-spanning segments in the intrinsic proteins that constitute the channel subunits (Kukuljan, Labarca & Latorre, 1995). K^+ channels whose subunits contain six membrane-spanning segments are voltage-regulated and are activated by membrane depolarization. In contrast, two membrane-spanning segments comprise subunits of channels that rectify inwardly, and, hence, are open at the magnitude of the resting transmembrane voltage.

We do not know the extent to which these respective K^+ channel families are involved in cell growth regulation. Voltage-gated K^+ channels in T lymphocytes function partly in the elaboration and secretion of interleukin 2 (IL-2), which acts as an autocrine growth factor and, thus, links K^+ channels to cell activation and proliferation (Chandy et al., 1984; Freedman, Price & Deutsch, 1992). Activation of B lymphocytes, on the other hand, involves Ca^{2+}-activated K^+ channels (Partiseti et al., 1992), and a *ras* transformation of 3T3 fibroblasts leads to upregulation of Ca^{2+}-activated K^+ current (Huang & Rane, 1993, 1994). A recent pharmacologic study of breast tumor cells excludes all voltage- and Ca^{2+}-activated K^+ channels in regulating cell growth and, instead, invokes the role of ATP-sensitive K^+ channels (Woodfork et al., 1995). It is unclear whether these differences reflect the phenotypic diversity among cell types and species. Nonetheless, it is evident that various membrane K^+ conductances affect cell growth (Wonderlin & Strobl, 1996; Dubois & Rouzaire-Dubois, 1993) and that the cellular mechanisms that link specific mem-

Correspondence to: R. Wondergem

Table 1. Ionic compositions of the bath (external) and pipette (internal) solutions

Solution	Na Gluconate (mM)	K Gluconate (mM)	$CaCl_2$ (mM)	$MgCl_2$ (mM)	Glucose (mM)	HEPES (mM)	EGTA (mM)	pH
External (bath)	135	5.4	1.8	2	10	5		7.41
Internal (pipette)		140	1	2		10	11	7.2
Internal (bath)		145	Variable (0.01–100 μM)	2		10	1	7.2

brane K^+ channels to the regulation of cell growth remain to be elucidated.

As an initial step in this direction, we aimed to determine the membrane K^+ currents and channels in a human bladder carcinoma cell line (HTB-9). These are relatively large cells that readily lend themselves to study by the patch clamp technique (Hamill et al., 1981). Moreover, they secrete various autocrine cytokines (Otsuka et al., 1991; Kaashoek et al., 1991). We show here that these cells contain at least two membrane K^+ currents and corresponding K^+ channels, one of which seems to play a principal role in mechanisms involved with control of cell proliferation (Wondergem et al., 1998). Preliminary reports of these findings have appeared elsewhere (Monen & Wondergem, 1996; Cregan et al., 1997).

Materials and Methods

Cell Culture

Human urinary bladder carcinoma cells of the HTB-9 cell line (Mochizuki et al., 1987) were obtained from ATCC (American Type Culture Collection, Rockville, MD) and were cultured in RPMI-1640 medium. The medium was supplemented with 5% fetal clone (HyClone, Logan, Utah) and 50 units/ml penicillin plus 0.05 mg/ml streptomycin (Sigma Chemical). Cells were cultured in 60 mm tissue culture plates in a water-jacketed incubator at 37°C, 5% CO_2, 95% air and 100% relative humidity. Confluent HTB-9 cells were passaged twice per week. This included washing cells twice with phosphate-buffered salt solution (PBS), incubating them for 10–20 min with porcine trypsin (1.2–2.5 mg/ml PBS), followed by aspiration, centrifugation (50 g), dilution with medium, and replating the cells. All organic chemicals were purchased from Sigma Chemical unless stated otherwise.

Whole-cell/Patch Clamp Technique

Cells were grown for 1–2 days on 4 × 4 mm sections of plastic coverslips that were transferred to an acrylic chamber (Warner, New Haven, CT) on the stage of an inverted microscope (Olympus IMT-2) equipped with Hoffman modulation contrast optics. Cells were superfused at room temperature with a standard external salt solution. The composition of this along with two internal solutions used throughout are given in Table 1.

Borosilicate glass capillaries (1.2 mm OD, 0.68 mm ID, type EN-1, Garner Glass, Claremont, CA) were cleaned in a sonicator and dried in a convection oven at 90°C. Patch pipettes (3–8 MΩ) were fabricated from the cleaned glass with a Brown-Flaming horizontal micropipette puller (P-87, Sutter Instruments, San Rafael, CA). These were coated to within 0.5 mm of the tip with a polystyrene base coil dope (Polyweld 912, Amphenol), and tips were heat-polished prior to use. A micromanipulator (MO-202, Narishige, Tokyo) was used to position pipettes. Ag/AgCl half-cells constituted the electrodes, and an agar bridge (4% in external solution) connected the reference electrode to the bath solution.

The whole-cell configuration plus outside-out and inside-out membrane patches were obtained by standard patch clamp technique (Hamill et al., 1981). Internal gluconate solutions were adjusted to contain various free $[Ca^{2+}]$ (Chang, Hsieh & Dawson, 1988) or other agents. Channel open probabilities were computed from channel current data obtained from 30–45 sec readouts taken at stated pipette potentials and bath Ca^{2+} or inhibitor concentrations.

Membrane currents were measured with a patch clamp amplifier (Axopatch 1-D, Axon Instruments, Foster City, CA) with the lowpass, Bessell filtering (-3 dB) set at 2kHz. Signals from the patch clamp amplifier fed into both a DAS 501 unitary gain PCM recorder (Dagan, Minneapolis, MN) and a DMA-1 digital interface connected to a 486-SX computer equipped with PCLAMP6 software (Axon Instruments). Recordings on both the PCM recorder and computer were sampled at 22 kHz.

Computations and Statistical Methods

Differences among means were determined by ANOVA and Student-Newman-Keuls test at $P < 0.05$. Channel open probability (P_o) was computed as:

$$P_o = \left(\sum_{n=1}^{N} P_n \right) / N$$

where P_n is the probability that n channels are open and was calculated as the amount of time in the open state divided by the total record time for each unitary current level. The summation of the values or P_n were then divided by the total number of channels (N) in the patch. The number of channels in a patch was determined from modal frequency distributions of channel current. In instances where the number of channels in a patch could not be determined accurately, total open probability (NP_o) was computed from pClamp event-list files by the analysis program of Sui, Chan & Logothetis (1996).

Membrane conductances and potassium channel conductances were calculated by using a least squares linear fit of the current-voltage

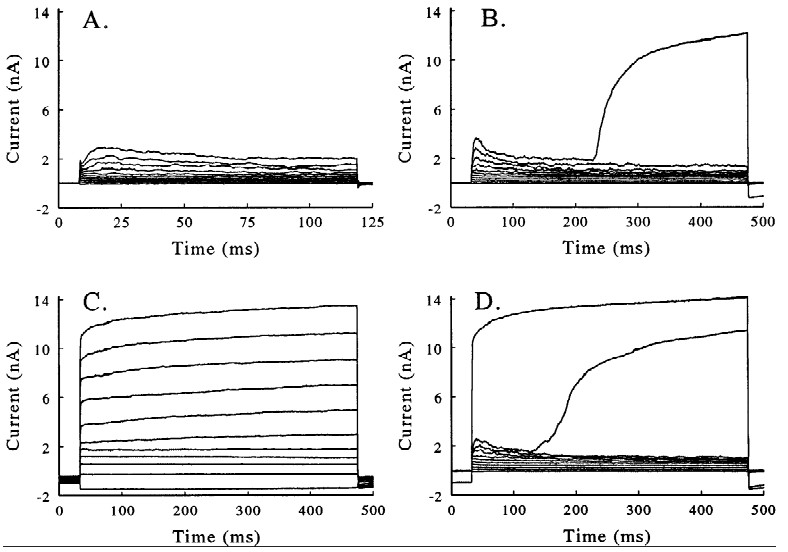

Fig. 1. Whole-cell voltage clamp recordings taken of a single human bladder tumor (HTB-9) cell. Voltage clamp was in consecutive 20-mV increments from −100 to 100 mV. (*A*) Voltage pulses of 110 msec duration. (*B*) Voltage pulses of 450 msec duration. (*C*) Voltage pulses of 450 msec duration with this protocol applied within 5 sec of the clamp protocol shown in *B.* (*D*) Voltage pulses of 450 msec duration with the protocol applied 5 min after the clamp protocol shown in *C.* Pipette: internal solution with 0.01 μM Ca^{2+}; bath: external solution.

curves for whole-cell and single channel patches. Unless stated otherwise, whole-cell conductances were computed from point data taken at the mid-duration of the voltage pulses. Whole-cell conductance was normalized by dividing by the measured whole-cell capacitance to obtain specific conductance.

RESULTS

Whole Cell Electrical Properties of HTB-9 Cells

Glass micropipettes, fabricated with a tip diameter of approximately 1 μm, had resistances that ranged from 3 to 8 MΩ when submerged in the bath. Seal resistance, ranging from 2–63 GΩ (mean = 7.5 ± 0.9 GΩ, n = 79), formed readily in flattened cells in spite of numerous filopodia as seen by scanning electron microscopy (P.H. Schmidt and S.K. Curtis, *unpublished observation*). The zero-current cell membrane voltage, V_m, obtained immediately after accessing the intracellular compartment, was −53 ± 4.9 mV (n = 15). The whole-cell capacitance was 20 ± 1.1 pF (n = 60); the series access resistance was 15.8 ± 1.4 MΩ (n = 60); and the whole-cell resistance was 404 ± 55 MΩ (n = 60). As the contents of the pipette dialyzed the cell, the zero-current membrane voltage increased to −75 mV, in approximation of the computed K^+ potential (E_K) of −85 mV. Consequently, the holding potential for most subsequent whole-cell measurements was set at −70 mV. Slope conductances of *I–V* plots obtained from steady current in the middle of the voltage pulses either were linear throughout or were linear in the range of negative transmembrane potential (*not shown*). The mean specific conductance (at −70 mV hold. pot.) of cells dialyzed with internal medium containing 0.01 μM Ca^{2+} was 0.56 ± 0.09 nS/pF (n = 11).

HTB-9 cells showed modest activation of outward whole-cell current at positive intracellular potentials of 110-msec duration, Fig. 1*A.* Figure 1*B* shows the response of the same cell to a voltage clamp of longer (450 msec) duration. The 100-mV voltage pulse activated a large outward current midway through the clamp interval, which yielded a tenfold increase in outward current. Figure 1*C* shows the response of the same cell to an immediate (within 5 sec after the clamp shown in Fig. 1*B*) repetition of the voltage clamp protocol. Now the increase in membrane current was evident at all voltages. Figure 1*D* shows the current response of the same cell to the voltage clamp 5 m following the clamp shown in Fig. 1*C.* By this time, the current had declined to the preactivation level; however, reactivation occurred midway through the 450-msec voltage pulse at 80 mV, and it also was evident throughout the clamp at 100 mV.

To ascertain more clearly the voltage-dependence (irrespective of time) for activation of outward current in HTB-9 cells, short duration (~60 msec) voltage pulses from −100 to 80 mV were repeated in the same cell at various holding potentials ranging from −70 to 20 mV, Fig. 2. Current activation and increased slope conductance during the voltage clamp protocol was evident at holding potentials of −10 and 20 mV, Fig. 2*B* and *C.* This activation reversed almost completely when the holding potential returned to −70 mV, Fig. 2*D.*

These measurements were repeated at various holding potentials to determine the membrane voltage at which the activation of outward current occurred. Changing the holding potential in 20-mV increments from −70 to 30 mV resulted in the specific conductances plotted by the *dashed line,* Fig. 3. Activation of outward current often occurred between −20 and −10 mV. Nonetheless, the large variation in measurements obtained at holding potentials of −10 and 10 mV resulted because

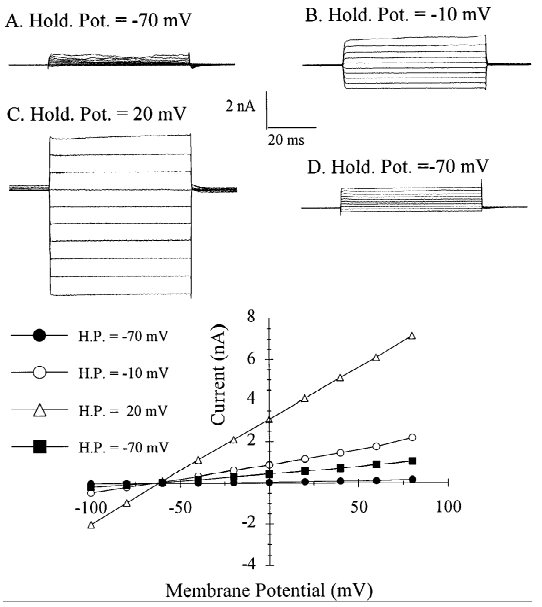

Fig. 2. Effect of altered holding potentials on whole-cell voltage clamp recordings taken from a human bladder tumor (HTB-9) cell. Voltage clamps were in consecutive 20-mV increments from −100 to 80 mV, and they were repeated at various holding potentials (HP): (*A*) HP = −70 mV. (*B*) HP = −10 mV. (*C*) HP = 20 mV. (*D*) HP = −70 mV. *Bottom.* Current-voltage plots taken from the voltage clamp protocols shown in *A–D.* Pipette: internal solution with 0.01 μM Ca^{2+}; bath: external solution.

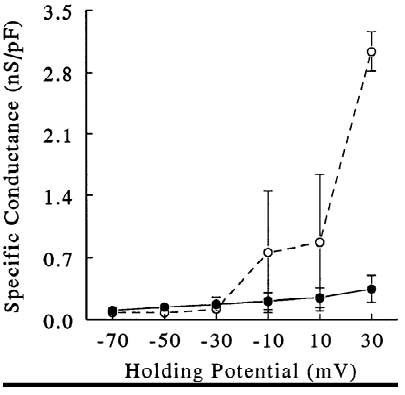

Fig. 3. HTB-9 whole-cell voltage clamp specific conductance plotted *vs.* cell holding potential, HP. Specific conductances were obtained from voltage clamp protocols (−100 to 80 mV) similar to those shown in Fig. 1. ○, *Dashed line:* Cell dialyzed with 0.01 μM Ca^{2+}. ●, *Solid line:* Cell dialyzed with nominally Ca^{2+}-free internal solution. Bath: external solution.

current activation did not occur in every cell at these voltages. However, the holding potential of 30 mV always activated outward current. This activation of outward current did not occur when the protocol was repeated using patch pipettes filled with Ca^{2+}-free internal solution, *solid line* in Fig. 3.

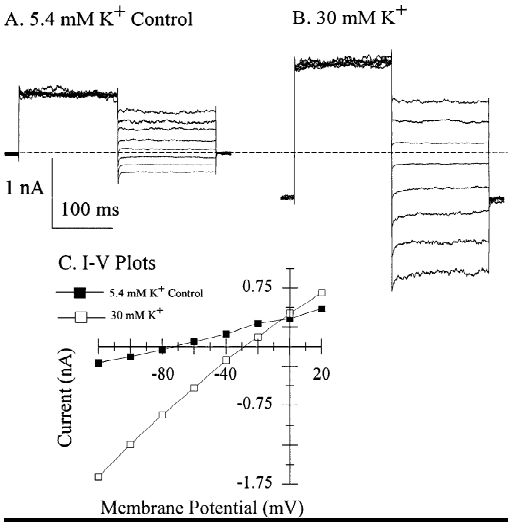

Fig. 4. Instantaneous current-voltage relationship following voltage-activation of a HTB-9 cell. Whole-cell voltage clamp recordings taken of a HTB-9 cell. Each voltage clamp protocol began with an activation voltage step to 60 mV, followed by consecutive repolarizing voltage steps in 20-mV increments beginning at −120 mV and ending at 20 mV. Pipette was filled with internal solution containing 1 μM Ca^{2+}. (*A*) Bath solution = 5.4 mM K^+. (*B*) Bath solution = 30 mM K^+. (*C*) Current-voltage plots (*I–V*) taken immediately after the application of the hyperpolarizing voltage pulses in *A* and *B.*

An instantaneous current-voltage relationship following voltage activation was used to ascertain whether the voltage-activated outward current was attributable to K^+. Here the cell was first voltage clamped to 60 mV followed by consecutive repolarizing voltage steps in 20-mV increments beginning at −120 mV and ending at 20 mV. This was done first with the external potassium concentration, $[K^+]_o$ = 5.4 mM, Fig. 4*A*, then repeated after switching to $[K^+]_o$ = 30 mM, Fig. 4*B.* The whole-cell currents, which were taken immediately after switching from the 60-mV pulse, were plotted in Fig. 4*C.* The reversal potentials were in fair agreement with the values of −84 and −40 mV predicted for $[K^+]_o$ of 5.4 and 30 mM, respectively. The membrane slope conductance increased at $[K^+]_o$ = 30 mM compared with that at $[K^+]_o$ = 5.4 mM, and there was modest inward rectification at $[K^+]_o$ = 30 mM for voltages more negative than −40 mV. *I–V* linearity returned along with a −70 mV reversal potential with restoration of 5.4 mM $[K^+]_o$ (*not shown*).

The effect of charybdotoxin (ChTx) and iberiotoxin (IbTx) on the voltage-activated outward current confirmed the presence of Ca^{2+}-activated K^+ currents in HTB-9 cells, Fig. 5. In each case, HTB-9 cells were voltage-clamped from −100 to 80 mV in 20-mV increments. Under control conditions this was done first at a holding potential of −70 mV (inactive) and then at a holding potential of 20 mV (active). This was repeated in cells treated with either 100 nM ChTx or 50 nM IbTx.

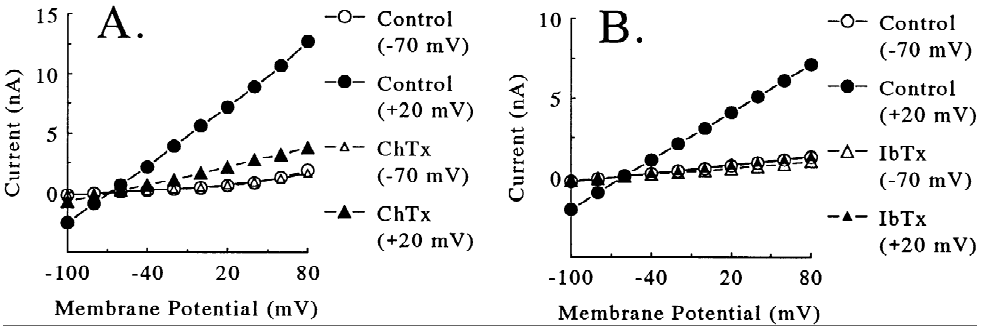

Fig. 5. Effect of scorpion venom peptides on whole-cell currents from HTB-9 cells. *I–V* plots were obtained from whole-cell voltage clamp of HTB-9 cells at inactive HP (−70 mV) and at activated HP (+20 mV), before (control) and after addition of charybdotoxin (ChTx; 100 nM) and iberiotoxin (IbTx; 50 nM). Pipette: internal solution; bath: external solution. Numbers in parentheses indicate the holding potential.

The results show that both IbTx and ChTx inhibit voltage-activated outward current in HTB-9 cells, Fig. 5.

The inward rectification of whole cell current recorded with high $[K^+]_o$, Fig. 4, prompted us to consider K^+ conductances in addition to the voltage-activated Ca^{2+}-dependent K^+ current. Addition of either $BaCl_2$ (1 mM) or quinine (100 μM) reduced whole-cell slope conductances, Table 2. Ba^{2+} and quinine, however, are broad acting K^+ channel inhibitors. Thus, we measured the effect of glibenclamide on whole-cell current, in an effort to determine whether the sulfonylurea receptor-linked K^+ channel contributes to this current. Glibenclamide (50 μM) inhibited whole-cell current during short duration (75 msec) voltage pulses, Fig. 6*A–C*, and Table 2. All cells tested responded to glibenclamide treatment (50 μM) with a decrease in whole-cell current if the pipette contained 1 μM ATP. However, whole cell current did not change in response to 50-μM glibenclamide when pipettes were filled with 1 mM ATP (*not shown).*

Table 2. Effects of K^+ channel blockers on whole cell specific conductance of HTB-9 cells

K^+ Channel blocker	Specific conductance (nS/pF) Control	Specific conductance (nS/pF) After inhibitor
Glibenclamide (50 μM)	0.65 ± 0.14 (4)	0.27 ± 0.03 (4)*
$BaCl_2$ (1 mM)	0.70 ± 0.13 (3)	0.30 ± 0.04 (3)*
Quinine HCl (100 μM)	0.90 ± 0.03 (3)	0.62 ± 0.08 (3)*

* Differs from control value, $P < 0.05$.
Pipette: internal solution; bath: external solution. Mean ± SE (*n*) of paired measurements.

Membrane Channel Properties of HTB-9 Cells

Current measurements recorded in response to voltage ramps (100 to −60 mV membrane potential, 3-sec interval) applied to inside-out patches demonstrated the voltage- and Ca^{2+}-dependence of large-conductance membrane K^+ channels, Fig. 7. Channel conductance was 214 ± 3.9 pS ($n = 3$). Channel activity in a single patch increased with the concentration of free Ca^{2+} in the bath from 0.01 to 100 μM, and it decreased on restoration of 0.01 μM Ca^{2+}, Fig. 7. Open probabilities (P_o) of this K_{Ca} channel increased with the magnitude of positive transmembrane voltage and with free $[Ca^{2+}]_i$, Fig. 8. P_o recorded from inside-out patches decreased to zero or near zero by addition to the bath of either Ba^{2+} (1 mM), quinine (100 μM) or TEA (10 mM), and this inhibition reversed immediately on washout (*not shown).*

We also examined the effects of ChTx and IbTx on K_{Ca} channel activity in outside-out patches, since these inhibitors bind to the channel on the outside of the membrane (Garcia et al., 1995). Voltage ramps from −60 to 100 mV (membrane potential) were applied to outside-out membrane patches from HTB-9 cells before, during, and after addition of either ChTx or IbTx to the external bathing medium. $[Ca^{2+}]_i$ in the pipette was 0.01 μM. Channel activity was evident only at positive membrane potentials ranging from approximately 0–60 mV, Fig. 9, which is consistent with the behavior of K_{Ca} channel at this $[Ca^{2+}]$. Both ChTx and IbTx at 50 nM abolished channel activity, which was restored on washout of the inhibitors.

A smaller conductance K^+ channel showed inward rectification during on-cell recordings, Fig. 10*A.* Conductance at negative transmembrane potential during on-cell patch measurements was 145 ± 13 pS ($n = 4$). This was an approximation, because the total transmembrane voltage comprised the pipette potential plus the estimated V_m of −53 mV. Channel conductance measured at positive V_m in detached inside/out patches, Fig. 10*B*, was 21 ± 1 pS ($n = 3$). This channel displayed neither the voltage- nor Ca^{2+}-dependence of the K_{Ca} channel. Apamin (100 nM) had no affect on the activity of this channel. In contrast, $BaCl_2$, added to the bath (2 mM) for 1

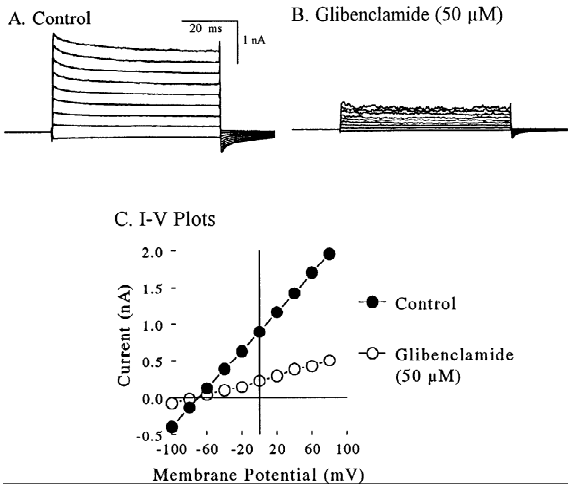

Fig. 6. Effect of glibenclamide on whole-cell currents of HTB-9 cells. Voltage clamp was in consecutive 20-mV increments from −100 to 80 mV. Holding potential = −70 mV, and the pipette was filled with internal solution + ATP (1 μM). (*A*) Whole-cell currents in untreated cell (control). (*B*) Whole-cell current in same cell in *A* after 2-min treatment with glibenclamide (50 μM). (*C*) *I–V* plots taken from the voltage clamp protocols in *A* and *B.*

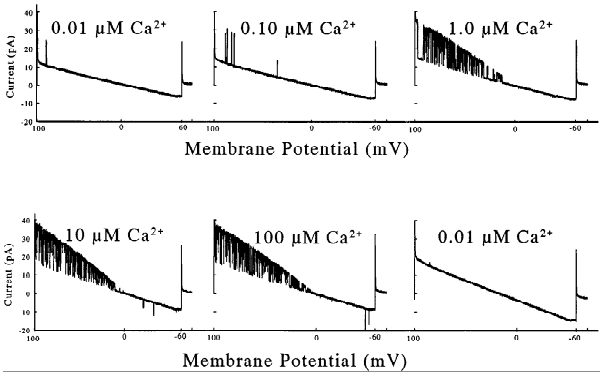

Fig. 7. Effect of $[Ca^{2+}]$ on K^+ channel activity. Channel currents recorded from inside-out patches during voltage ramps from −100 to 60 mV (pipette potential over a 3-sec interval) in bath solutions containing various free $[Ca^{2+}]$ ranging from 0.01 μM to 100 μM and computed according to Chang, Hsieh and Dawson (1988). All records were from the same patch. Symmetrical transmembrane $[K^+]$; Pipette: internal solution; bath: internal solution.

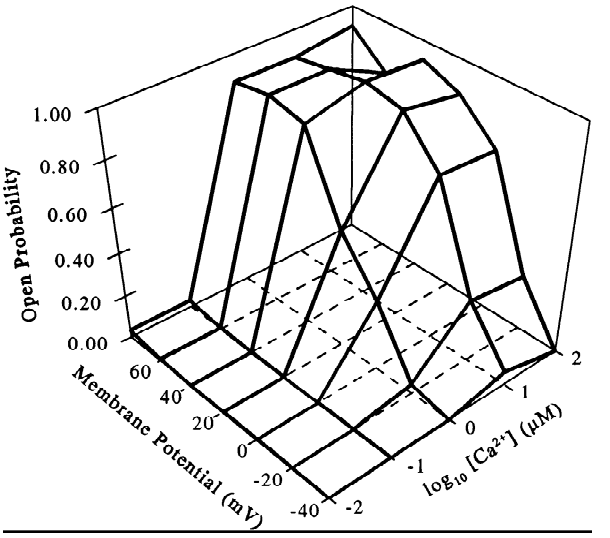

Fig. 8. K^+ channel open probability, P_o, plotted *vs.* $\log_{10}$ $[Ca^{2+}]$ and pipette potential. Data were recorded from an inside-out patches obtained from HTB-9 cells. Pipette: external solution; Bath: internal solution. P_os were computed from analysis of 45 sec of recording corresponding to the conditions of each coordinate.

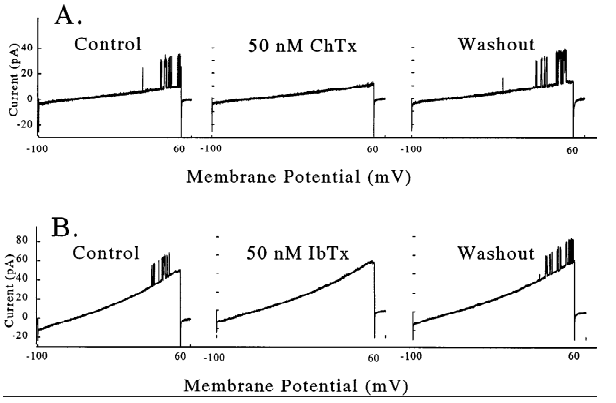

Fig. 9. Outside-out channel current recorded during voltage ramps from −100 to 60 mV (membrane potential over a 3-sec interval). Before, during and after addition of charybdotoxin (ChTx; 50 nM) and iberiotoxin (IbTx; 50 nM). Pipette: internal solution; bath: external solution.

min while the outside-out patch was held at −70 mV, eliminated all subsequent channel activity during voltage ramps from −100 to 100 mV (*not shown*).

This channel also was inhibited by ATP. An inside-out patch was used for results shown in Fig. 11, and the patch pipette was filled with internal solution (140 mM K^+). Voltage ramps from −100 to 100 mV were applied over 3 sec to obtain results in each section. In Fig. 11*A* the bath was filled with external medium and channel activity was evident only at negative transmembrane potentials. When the bath solution was exchanged with an internal solution that resulted in symmetrical transmembrane K^+ concentrations of 140 mM, channel activity occurred at both positive and negative transmembrane potentials, Fig. 11*B.* Increasing bath concentration of ATP from 1 μM to 2 mM abolished channel activity, Fig. 11*C.* Fig. 11*D–F* show sequential restoration, inhibition, and restoration of channel activity with corresponding changes in bath ATP concentration. The apparent inward rectification, which was evident from on cell recordings, never occurred during voltage ramps applied to the inside/out patches.

Since ATP-regulated K^+ channels comprise a class

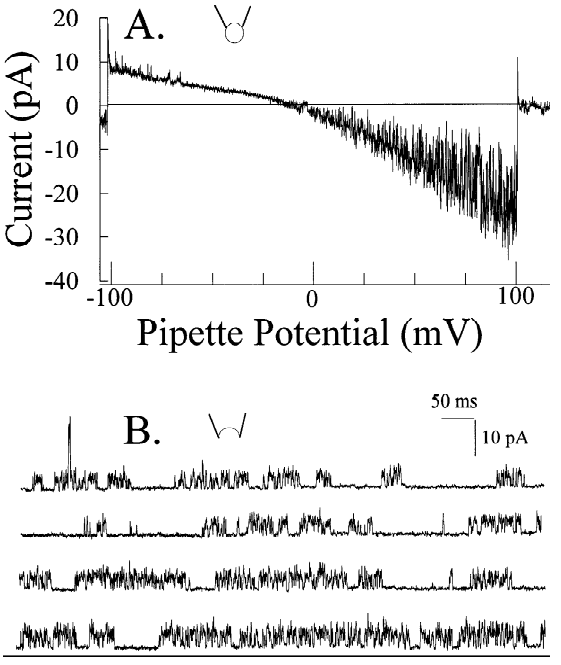

Fig. 10. Inwardly rectifying K^+ channel from an HTB-9 cell. (*A*) On-cell patch current recording of HTB-9 cell during voltage ramp from −100 to 100 mV (pipette potential over a 3-sec interval). Pipette: internal solution; bath: external solution. (*B*) Inside-out patch current recording taken at 60 mV (membrane potential). Pipette: external solution; bath: internal solution with 0.01 μM Ca^{2+}. Trace shows activity of two channels. Large channel current in the record is one opening of K_{Ca}. Gating of this channel increased markedly in this patch by raising $[Ca^{2+}]$ (*not shown*).

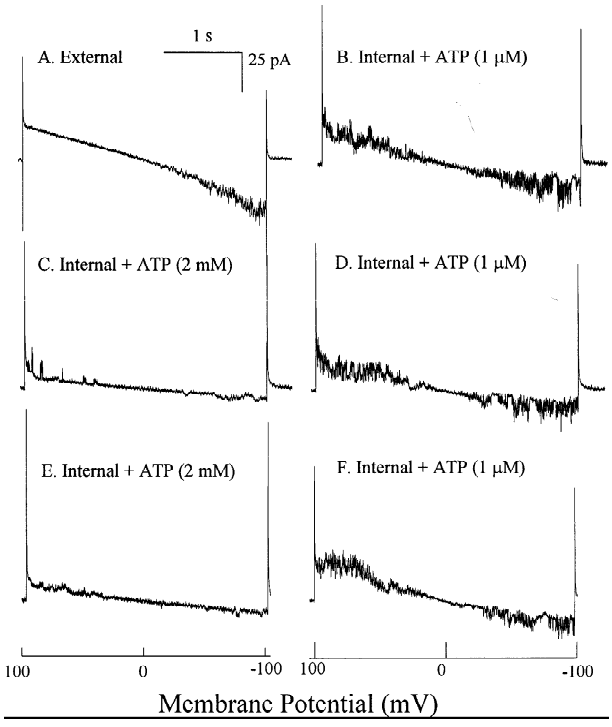

Fig. 11. Effect of ATP on K^+ channel recordings from inside-out patches obtained from HTB-9 cells. Voltage ramps were from 100 to −100 mV (membrane potential over a 3-sec interval) for each trace. Pipette contained internal solution. All traces are from the same patch with sequential bath solutions of: (*A*) External solution; (*B*) Internal solution + 1 μM ATP; (*C*) Internal solution + 2 mM ATP; (*D*) Internal solution + 1 μM ATP; (*E*) Internal solution + 2 mM ATP; (*F*) Internal solution + 1 μM ATP.

of channels linked to the sulfonylurea receptor (Inagaki et al., 1995), we determined whether a sulfonylurea compound inhibited channel activity. Glibenclamide (50 μM added to the bath) markedly reduced K^+ channel activity in an inside-out patch compared with control, Fig. 12*A* and *B*. The open probability of this K^+ channel decreased with the dose of glibenclamide, Fig. 13. The IC_{50} was 46 μM, and it was computed from a best fit sigmoidal plot of P_o *vs.* the $\log_{10}$ μM-dose of glibenclamide (*not shown*). The reduction of channel activity by glibenclamide was not immediate, however, and approximately 2 min comprise the breaks between the sequential histograms of open probability in Fig. 13. Channel activity returned over 10 min following three washes of the bath.

Activation of K_{ATP} channels was also evident when diazoxide was added to an inside-out patch, Fig. 14. Voltage ramps from −100 to 100 mV were applied over 3 sec during each measurement. Figure 14*A* shows a patch in which there was no channel activity. However, channel activity in the same patch was very evident at both negative and positive pipette potentials immediately after addition of diazoxide (100 μM) to the bath, Fig. 14*B*. This reversed on washout of the diazoxide,

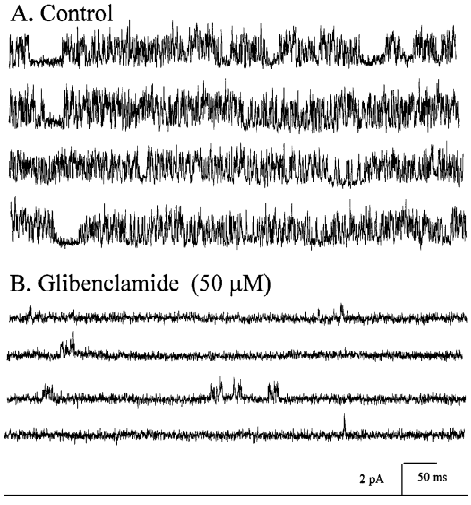

Fig. 12. Effect of glibenclamide on K^+ channel activity in an HTB-9 cell. Current recordings from an inside-out patch obtained from a HTB-9 cell. Membrane potential = 60 mV. Pipette: internal solution; bath: internal solution. (*A*) Control; (*B*) 2-min after addition of glibenclamide (50 μM).

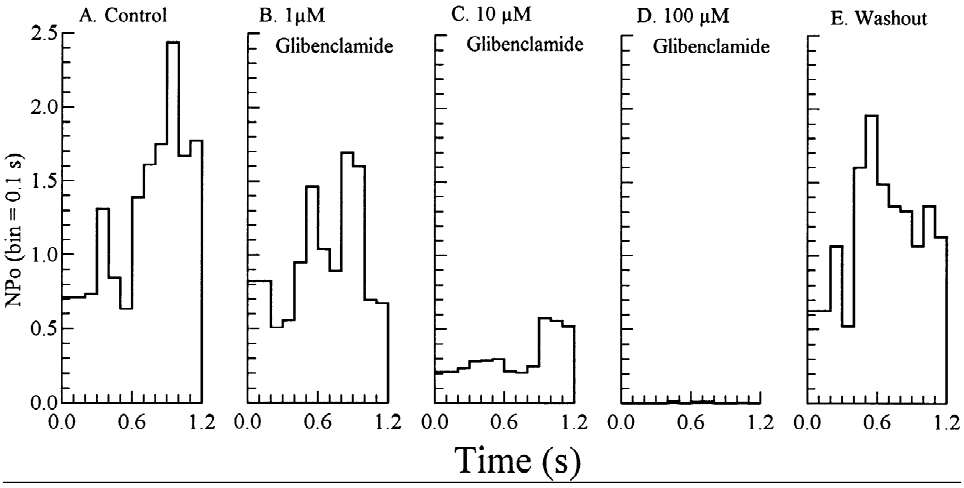

Fig. 13. Effect of glibenclamide on K^+ channel total open probability in an inside-out patch obtained from a HTB-9 cell. Symmetrical 140-mM K^+ solutions were in the pipette and bath. Membrane potential = −60 mV. Total open probability, the product of the number of channels (*N*) times open probability (P_o), was plotted vs. time (1.2 sec) for sequential glibenclamide concentrations in the bath comprising: (*A*) O mM (Control); (*B*) 1 μM glibenclamide; (*C*) 10 μM glibenclamide; (*D*) 100 μM glibenclamide; (*E*) 0 mM (Washout).

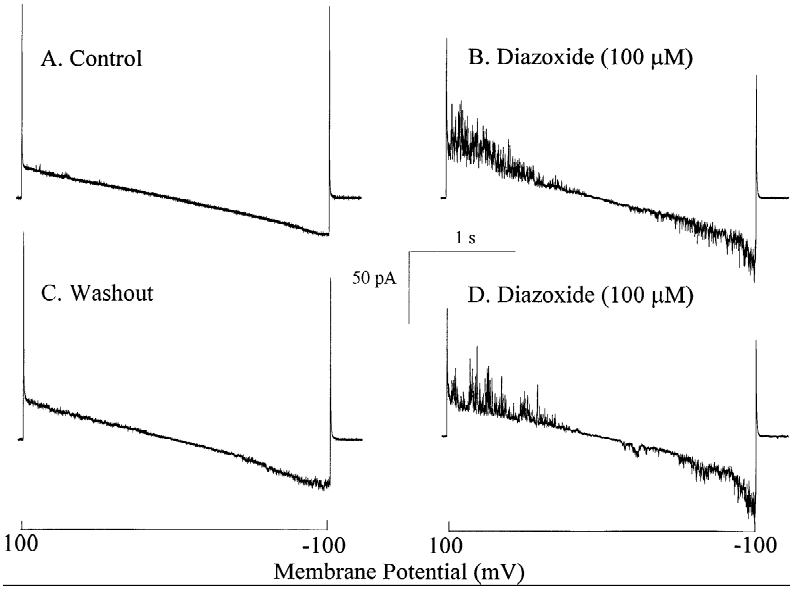

Fig. 14. Effect of diazoxide on K^+ channel recordings from inside-out patches obtained from HTB-9 cells. Voltage ramps were from 100 to −100 mV (membrane potential over a 3-sec interval) for each trace. Pipette contained internal solution. All traces were obtained from the same patch with sequential bath internal (plus 1 μM ATP) solutions of: (*A*) Control; (*B*) plus diazoxide (100 μM); (*C*) Washout control; (*D*) plus diazoxide (100 μM).

Fig. 14*C*, and readdition of diazoxide restored the channel activity, Fig. 14*D*.

Discussion

At least two membrane K^+ currents and corresponding channels contribute to the total plasma membrane K^+ conductance (gK) of HTB-9 cells. These are the Ca^{2+}- and voltage-activated K^+ channel (K_{Ca}) and the glibenclamide-sensitive ATP-regulated K^+ channel (K_{ATP}). Together they provide loci whereby changes in the cytoplasmic concentrations of either Ca^{2+} or ATP can affect membrane gK and the transmembrane potential (V_m).

Inhibition of voltage-activated outward K^+ currents, either by dialyzing the cells with a Ca^{2+}-free pipette filling solution or by addition of ChTx and IbTx, demonstrates the Ca^{2+}-dependence of this K^+ current. However, the time-dependence for both voltage-activation and recovery of this outward K^+ current suggests that regulation of $[Ca^{2+}]_i$ involves intercurrent cellular mechanisms besides voltage. We have not determined what these are, nor have we determined the extent to which this phenomenon depends on extra- vs. intracellular Ca^{2+}.

The properties of the K_{Ca} channels in HTB-9 cells are consistent with those reported previously for other cell types. The single channel conductance is well within the range of values reported for Ca^{2+}-activated K^+ channels (Latorre et al., 1989). Inhibition of K^+ channels in outside/out patches by ChTx and IbTx also identified the channels as K_{Ca} channels, since both peptides are well-known blockers of K_{Ca} (Garcia et al., 1995). The inhibition by IbTx in particular is selective for the large-conductance Ca^{2+}-activated K^+ channel (Giangiacomo, Garcia & McManus, 1992). The profile of the channel open probability *vs.* the internal Ca^{2+} concentration and transmembrane voltage was similar to the profile reported by Barrett, Magleby and Pallota (1982) for the Ca^{2+}-activated K^+ channels in cultured rat skeletal muscle.

The instantaneous current voltage relationship following voltage activation were consistent with those expected of a K^+ current. The reversal potentials approximated those prediced for K^+-selective membranes at the respective $[K^+]_o$ of 5.4 mM and 30 mM. In addition, the slope conductance increased with $[K^+]_o$, which also is consistent with membrane K^+ currents (Hagiwara, Miyazaki & Rosenthal, 1976). The moderate inward rectification of the whole-cell *I–V* curve at 30 mM $[K^+]_o$, and the inward rectification of a lower conductance K^+ channel in the cell-attached patch mode, implies the existence of membrane K^+ currents besides those attributable to the K_{Ca} channels.

We conclude that this additional K^+ current in HTB-9 cells is linked to the sulfonylurea receptor (SUR), because glibenclamide reduced membrane K^+ current and it inhibited K^+ channel activity in a dose-dependent manner. We note, however, that the IC_{50} of 46 μM for the latter effect was far greater than the K_i estimated for pancreatic β-cells (Inagaki et al., 1996). Hence, the isoform of the SUR in HTB-9 cells is more like either that of SUR2 reported for skeletal and cardiac muscle (Inagaki et al., 1996) or that of a novel cardiac SUR that associates with a smooth muscle type ATP-sensitive K^+ channel (Isomoto et al., 1996).

Inhibition of the lower conductance K^+ channel by millimolar concentrations of ATP and its activation by diazoxide provide further evidence of the presence of K_{ATP} in HTB-9 cells. We have no ready explanation as to why inwardly rectifying properties of this channel were not apparent during voltage ramps applied to inside/out patches that were bathed with symmetric K^+ solutions. Cytoplasmic factors, such as polyamines, have been reported to contribute to the intrinsic gating properties of some inwardly rectifying K^+ channels (Ficker et al., 1994). We conclude that the inwardly rectifying property of this channel and membrane current requires an intact cell.

In summary, these findings show that HTB-9 cells have two predominant membrane K^+ channels and corresponding membrane currents: a 214 pS Ca^{2+}- and voltage-activated K^+ channel (K_{Ca}) and a sulfonylurea-receptor linked K^+ channel that also is inhibited by mM-concentrations of ATP. Both provide loci whereby cellular metabolites and signaling ions can affect the K^+ conductance and V_m of the plasma membrane.

We thank S.K. Curtis for performing electron microscopy, J.L. Sui and D.E. Logothetis for computer software to determine channel total open probability, and D.C. Dawson for computer software to calculate free Ca^{2+} concentration. This work was supported in part by grants to R.W. from the National Institute on Alcohol Abuse and Alcoholism and the Cardiovascular Research Institute of East Tennessee State University, and a scholarship to S.H.M. from TN-SBR.

References

Amigorena, S., Choquet, D., Teillaud, J.-L., Korn, H., Fridman, W.H. 1990. Ion Channel blockers inhibit B cell activation at a precise stage of the G_1 phase of the cell cycle. Possible involvement of K^+ channels. *J. Immunol.* **144:**2038–2045

Barrett, J.N., Magleby, K.L., Pallotta, B.S. 1982. Properties of single calcium-activated potassium channels in cultured rat muscle. *J. Physiol.* **331:**211–230

Chandy, K.G., DeCoursey, T.F., Cahalan, M.D., McLaughlin, C., Gupta, S. 1984. Voltage-gated potassium channels are required for human T lymphocyte activation. *J. Exp. Med.* **160:**369–385

Chang, D., Hsieh, P.S., Dawson, D.C. 1988. Calcium: a program in basic for calculating the compositions of solutions with specified free concentrations of calcium, magnesium and other divalent cations. *Comput. Biol. Med.* **18:**351–366

Cregan, M., Strickler, L., Miller, R., Suttles, J., Wondergem, R. 1997. Effect of glibenclamide on the growth of human bladder tumor (HTB-9) cells. *Biophys. J.* **72:**A412

Dubois, J.-M., Rouzaire-Dubois, B. 1993. Role of potassium channels in mitogensis. *Prog. Biophys. Molec. Biol.* **59:**1–21

Ficker, E., Taglialatela, M., Wible, B.A., Henley, C.M., Brown, A.M. 1994. Spermine and spermidines as gating molecules for inward rectifier K^+ channels. *Science* **266:**1068–1072

Freedman, B.D., Price, M.A., Deutsch, C.J. 1992. Evidence for voltage modulation of IL-2 production in mitogen-stimulated human peripheral blood lymphocytes. *J. Immunol.* **149:**3784–3794

Garcia, M.L., Knaus, H.-G., Munujos, P., Slaughter, R.S., Kaczorowski, G.J. 1995. Charybodotoxin and its effects on potassium channels. *Am. J. Physiol.* **269:**C1–C10

Giangiacomo, K.M., Garcia, M.L., McManus, O.B. 1992. Mechanism of iberiotoxin block of the large-conductance calcium-activated potassium channel from bovine aortic smooth muscle. *Biochemistry* **31:**6719–6727

Grinstein, S., Foskett, J.K. 1990. Ionic mechanisms of cell volume regulation in leukocytes. *Annu. Rev. Physiol.* **52:**399–414

Hagiwara, S., Miyazaki, S., Rosenthal, N.P. 1976. Potassium current and the effect of cesium on this current during anomalous rectification of the egg cell membrane of a starfish. *J. Gen. Physiol.* **67:**621–638

Hamill, O.P., Marty, A., Neher, E., Sakmann, B., Sigworth, F.J. 1981. Improved patch-clamp techniques for high-resolution current recording from cells and cell-free membrane patches. *Pflugers. Arch.* **39:**85–100

Huang, Y., Rane, S.G. 1993. Single channel study of a Ca^{2+}-activated K^+ current associated with *ras*-induced cell transformation. *J. Physiol.* **461:**601–618

Huang, Y., Rane, S.G. 1994. Potassium channel induction by the Ras/Raf signal transduction cascade. *J. Biol. Chem.* **269:**31183–31189

Inagaki, N., Gonoi, T., Clement IV, J.P., Noriyuki, N., Inazawa, J., Gonzalez, G., Aguilar-Bryan, L., Seino, S., Bryan, J. 1995. Reconstitution of I_{KATP}: an inward rectifier subunit plus the sulfonylurea receptor. *Science* **270:**1166–1170

Inagagki, N., Gonoi, T., Clement, J.P., Wang, C.Z., Aguilar-Bryan, L., Bryan, J., Seino, S. 1996. A family of sulfonylurea receptors determines the pharmacological properties of ATP-sensitive K^+ channels. *Neuron* **16:**1011–1017

Isomoto, S., Kondo, C., Yamada, M., Matsumoto, S., Higashiguchi, O., Horio, Y., Matsuzawa, Y., Kurachi, Y. 1996. A novel sulfonylurea receptor forms with BIR (Kir6.2) a smooth muscle type ATP-sensitive K^+ channel. *J. Biol. Chem.* **271:**24321–24324

Kaashoek, J.G., Mout, R., Falkenburg, J.H., Willemze, R., Fibbe, W.E., Landegent, J.E. 1991. Cyotokine production by the bladder carcinoma cell line 5637: rapid analysis of mRNA expression levels using a cDNA-PCR procedure. *Lymphokine Cytokine Res.* **10:**231–235

Kukuljan, M., Labarca, P., Latorre, R. 1995. Molecular determinants of ion conduction and inactivation in K^+ channels. *Am. J. Physiol.* **268:**C535–C556

Latorre, R., Oberhauser, A., Labarca, P., Alvarez, O. 1989. Varieties of calcium-activated potassium channels. *Annu. Rev. Physiol.* **51:**385–389

Mochizuki, D.Y., Eisenman, J.R., Conlon, P.J., Larsen, A.D., Tushinski, R.J. 1987. Interleukin 1 regulates hematopoietic activity, a role previously ascribed to hemopoietin 1. *Proc. Natl. Acad. Sci. USA* **84:**5267–5271

Monen, S.H., Wondergem, R. 1996. Calcium activated potassium channels in human bladder tumor cells. *Biophys. J.* **70:**A192

Nilius, B., Wohlrab, W. 1992. Potassium channels and regulation of proliferation of human melanoma cells. *J. Physiol.* **445:**537–548

Otsuka, T., Humphries, R.K., Hogge, D.E., Eaves, A.C., Eaves, C.J. 1991. Continuous activation of primitive hematopoietic cells in long-term human marrow cultures containing irradiated tumor cells. *J. Cell. Physiol.* **148:**370–379

Partiseti, M., Choquet, D., Diu, A., Korn, H. 1992. Differential regulation of voltage- and calcium-activated potassium channels in human B lymphocytes. *J. Immunol.* **148:**3361–3368

Sui, J.L., Chan, K.W., Logothetis, D.E. 1996. Na^+ activation of the muscarinic K^+ channel by a G-protein-independent mechanism. *J. Gen. Physiol.* **108:**381–391

Wondergem, R., Cregan, M., Strickler, L., Miller, R., Suttles, J. 1998. Membrane potassium channels and human bladder tumor cells. II. Growth properties. *J. Membrane Biol.* **161:**257–262

Wonderlin, W.F., Strobl, J.S. 1996. Potassium channels, proliferation and G1 progression. *J. Membrane Biol.* **154:**91–107

Woodfork, K.A., Wonderlin, W.F., Peterson, V.A., Strobl, J.S. 1995. Inhibition of ATP-sensitive potassium channels causes reversible cell-cycle arrest of human breast cancer cells in tissue culture. *J. Cell Physiol.* **162:**163–171